Available online at www.sciencedirect.com
ScienceDirect
Solid-State Electronics 52 (2008) 679–682
SOLID-STATE ELECTRONICS
www.elsevier.com/locate/sse

Ultraviolet Schottky detector based on epitaxial ZnO thin film

Dayong Jiang, Jiying Zhang *, Youming Lu, Kewei Liu, Dongxu Zhao, Zhenzhong Zhang, Dezhen Shen, Xiwu Fan

Key Laboratory of Excited State Processes, Changchun Institute of Optics, Fine Mechanics and Physics. Chinese Academy of Sciences, Changchun 130033, China

Received 10 April 2007; received in revised form 10 October 2007; accepted 18 October 2007
Available online 3 December 2007

The review of this paper was arranged by Prof. Y. Arakawa

Abstract

In this paper, we have prepared Schottky type ZnO metal–semiconductor–metal (MSM) ultraviolet (UV) detector. The structural, electrical, and optical measurements were carried out. The detector exhibited a peak responsivity of 0.337 A/W at 360 nm and the dark current was about 1 nA under 3 V bias. An ultraviolet–visible rejection ratio was obtained about more than four orders of magnitude from the fabricated detector. The 10–90% rise and fall time were 20 ns and 250 ns, respectively. We proposed that the detector had shown a gain, which was attributed to the trapping of hole carriers at the semiconductor–metal interface.

Keywords: Detector; ZnO; MSM

1. Introduction

Over the past few years, there has been increasing interest in ZnO as optoelectronic materials. ZnO is a wide direct bandgap material that is sensitive in the UV region. The large exciton binding energy of 60 meV and the wide bandgap energy of 3.37 eV at room temperature make ZnO a promising photonic material for applications such as lighting-emitting diodes, laser diodes and UV detectors [1–4]. Furthermore, ZnO also possess unique figures of merit, such as the availability of lattice-matched single-crystal substrates, low thin film growth temperatures (100–750 °C) [5], and radiation hardness [6], which are crucial for practical optoelectronic materials. Despite the challenges of reliable p-type doping of ZnO that hinder the realization of p–n junction-based devices, only MSM structured UV detectors with either Schottky or ohmic contacts were reported. However, a majority of them were based on ohmic junction which was photoconductive type [7–10]. Very long decay time and large dark current are the disadvantages of this type of UV detector, nearly all photoconductive type UV detectors exhibit high gain. As a result, photocurrent and optical power present nonlinearity and the capability of the device will degrade seriously. But Schottky type detectors are more attractive due to their high speed and low noise performance [11–14]. As is known, the fastest ZnO ultraviolet Schottky detector was reported by S. Liang. The photoresponse raise within 12 ns and fell to 66% of its peak value within 50 ns [12].

Schottky type ZnO MSM UV detector presents several attractive features that make it an ideal candidate for space application: very low dark current, large bandwidth, and short response time, extremely. The gain in the detector is always related to the trapping of hole carriers. In this work, ZnO thin films were grown by radio frequency magnetron sputtering on SiO_2 substrates. The MSM structure of the interdigitated Au-electrodes was fabricated by lithography and wet photoetching.

* Corresponding author.
E-mail address: zhangjy53@yahoo.com.cn (J. Zhang).

0038-1101/$ - see front matter © 2007 Elsevier Ltd. All rights reserved.
doi:10.1016/j.sse.2007.10.040

2. Experimental

Ultraviolet Schottky detector based on epitaxial ZnO thin film was fabricated through two steps: the preparation of ZnO thin films and the etching of the interdigitated Au-electrodes. The experimental procedure was as follows: First, before deposition, the Zinc (99.999) target was etched with diluted nitric acid to remove the contamination. The distance between the Zinc target and the SiO_2 substrate was 6 cm. The sputtering chamber was evacuated down to 3×10^{-4} Pa before introducing the sputtering gas. Ar and O_2 gases were introduced into the sputtering chamber through a set of mass flow controllers with the rates of 60 and 20 SCCM (standard cubic centimeter per minute), respectively. The working pressure in the chamber was kept at 1 Pa with an rf power of 150 W and the substrate temperature was controlled at about 400 °C. The rate of deposition is adjusted so as to have a film thickness of nearly 400 nm during the film growth for 60 min. Second, Au as a contact metal because of its comparatively high work function was deposited on ZnO thin films from a resistance evaporator under the pressure of 1×10^{-3} Pa. Following this, we chose the positive photoresist for photoetching due to it having an adhesively contact with the face of Au. The clear-cut MSM structure with interdigitated configuration was obtained by lithography and wet etching. It consists of 12 fingers at each electrode. The thickness of the Au-electrodes is 100 nm. The electrode fingers are 5 μm wide, 500 μm long, and with a pitch of 2 μm.

The surface topography of ZnO UV photodetector is characterized by scanning electron micrograph. The structure characterizations of the ZnO thin films are carried out by XRD using a D/max-RA X-ray spectrometer (Rigaku) with Cu Kα radiation of 0.154 nm. The optical absorption and transmission spectra are recorded using a Shimadzu UV-3101PC scanning spectrophotometer.

For the characterization of the detector which was biased with 3 V and having a load resistance of about 50 Ω, the photoresponse was performed by a 150 W Xe lamp and an amplifier, a pulsed Nd-YAG laser (355 nm, 10 ns) was used to measure the time response as the excitation source. The dark current was measured by Hall measurement system.

3. Results and discussion

Fig. 1 shows the X-ray diffraction pattern of ZnO thin film on SiO_2 substrate. The film shows a sharp peak at 34.4° which can be attributed to the ZnO (002) plane. No other peak is observed, which indicates the preferred orientation of the film. The micrographs of Au and ZnO are shown in Fig. 1b and c, respectively. Their surfaces are considerably smooth and compact after photoetching.

Fig. 2 shows the variations of $(\alpha hv)^2$ vs. hv of the detector. It is known that the correlation between absorption coefficient α and optical band gap E_g can be determined by the following equation [15]:

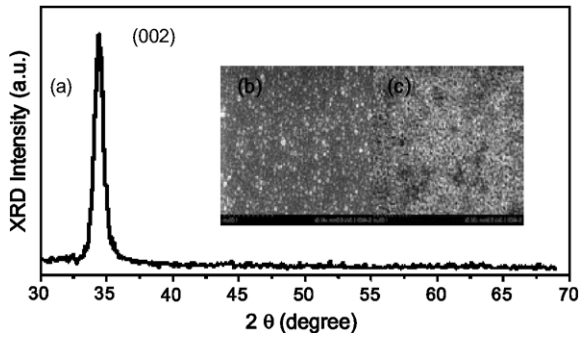

Fig. 1. (a–c) are the XRD spectra of ZnO thin film prepared on SiO_2, and the scanning electronic microscope picture of Au and ZnO, respectively.

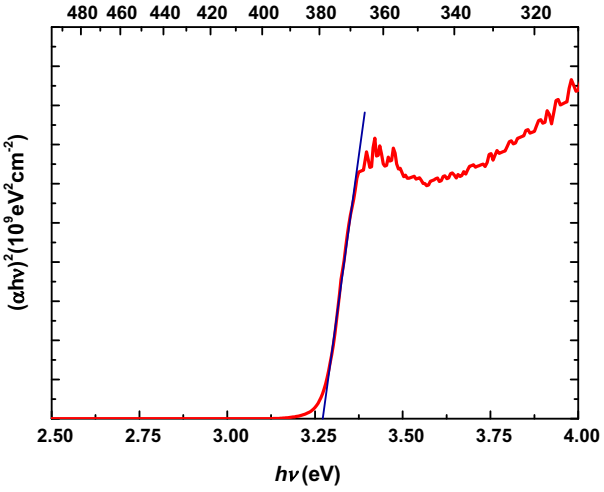

Fig. 2. Variations of $(\alpha hv)^2$ vs. hv of the detector.

$$(\alpha hv)^2 = A(hv - E_g) \tag{1}$$

where α is the absorption coefficient, A is a constant, and hv is photon energy. Hence, the optical band gap for the absorption peak can be obtained by extrapolating the linear portion of the plot of $(\alpha hv)^2$ vs. hv to $\alpha = 0$ as depicted in the inset of Fig. 2, E_g of ZnO thin film is about 3.27 eV.

In Fig. 3, is the I–V characteristics of ZnO MSM structure with interdigited configuration measured in dark and under 365 nm illumination are shown. The I–V curves indicate the Schottky behavior of Au on n-type ZnO contact, which corresponds to the large leakage resistance and the high quality of the contacts. The photocurrent under 365 nm illumination is obviously higher than the dark current. The dark current is only about 1 nA at 3 V bias. It is not more than 10 nA even when operating at 75 V bias. The fact is that the Schottky type detector presents very low dark current due to the high material resistivity and Schottky barrier height. The low dark current is helpful to enhance the detector's signal-to-noise (S/N) ratio since the shot noise, which exceeds the Johnson and $1/f$ noise if the operating frequency is not too low, is proportional to dark current [16]. The dark I–V curve takes on favorable

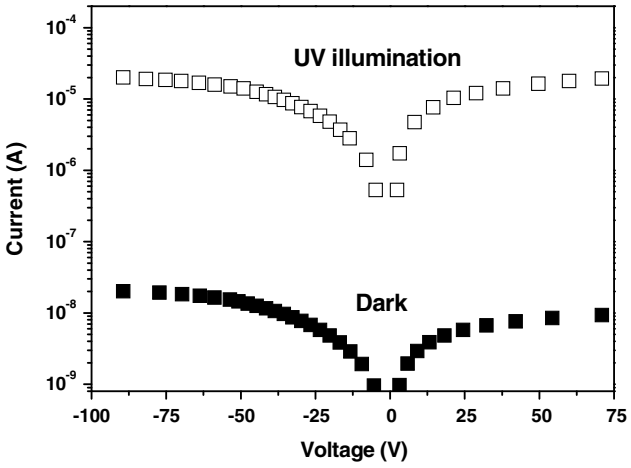

Fig. 3. *I–V* characteristics of ZnO MSM structure with interdigited configuration measured in dark and 365 nm illumination.

symmetrical characteristic when the bias voltage is not very large, demonstrating that the interdigited electrodes and the ZnO thin film are intact after photoetching. The breakdown voltage is higher than 100 V bias, which indicates that the voltage withstanding character of the ZnO UV detector is very good.

Fig. 4 presents the responsivity as a function of wavelength for ZnO UV detector. At 3 V bias, the peak of the responsivity occurred at around 360 nm. The UV-to-visible rejection was more than four orders of magnitude from 360 to 450 nm. It was found that the maximum responsivity of the detector was 0.337 A/W, which corresponds to the pitch of 2 μm. Ideal photovoltaic devices were not expected to exhibit gain [17]. However, the responsivity was very large, so we believe there was a big gain in the detector. This can be proved by the following formula [18]:

$$R_{\text{limit}} = \frac{e}{hv} \times \frac{S}{S+W} \tag{2}$$

where R_{limit} is the limited responsivity of photovoltaic detectors, S is the finger pitch, and W is the finger width. It was estimated that the R_{limit} (~0.103 A/W) was smaller than the responsivity (~0.337 A/W) at 360 nm. Thus the high responsivity was attributed to the large gain. The gain can be expressed in the form [19]

$$G = \frac{\tau}{\tau_{\text{tr}}} \tag{3}$$

where τ is the hole(minority) lifetime and τ_{tr} is the transit time. In our case, it is supposed that the gain in the detector is due to the hole traps at the semiconductor–metal interface. Below a certain operating voltage, the hole traps will capture the hole carriers of a definite magnitude. The smaller the pitch was, the larger the electric-field intensity was. So the recombination rate of electrons and holes will decrease. The electrons will be collected easily by passive electrodes. This is because the effect mass of the electrons was extremely light in comparison to the holes. While the bias voltage was not very large such as 3 V bias, there was not enough electric-field intensity, so the holes were still hard to collect in contrast to the electrons. As a result, the recombination between the electrons and the holes will reduce. So the hole carriers lifetime τ will be longer. Obviously, we obtain a big gain with the pitch of 2 μm. The responsivity R can be described as [19]

$$R = \eta g \frac{q\lambda}{hc} \tag{4}$$

where q, λ, h, and c are the electron charge, the incident wavelength, the Planck constant, and the speed of light, respectively. From Eq. (4), we can see that the high responsivity was caused by the big gain.

The response time of ZnO UV detector is shown in Fig. 5. The 10–90% rise and fall time were 20 ns and 250 ns, respectively. As far as I am concerned, it was faster than the response time which was reported by S. Liang who got 66% of the peak value [12]. The 20 ns rise time is limited by the excitation laser, which has a nominal pulse duration FWHM of 10 ns. For high performance of the ZnO thin

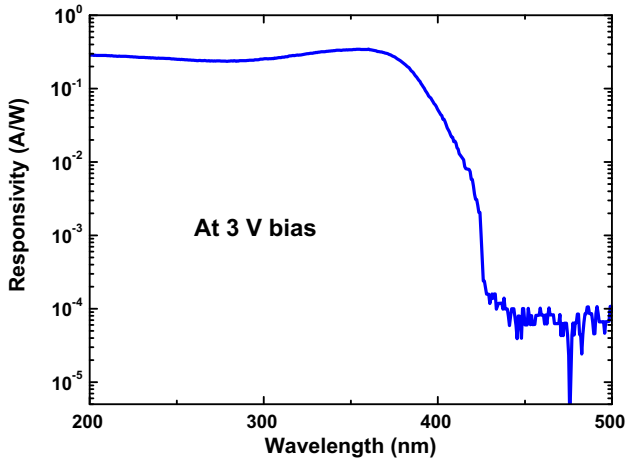

Fig. 4. The responsivity as a function of wavelength for ZnO UV detector with the pitch of 2 μm.

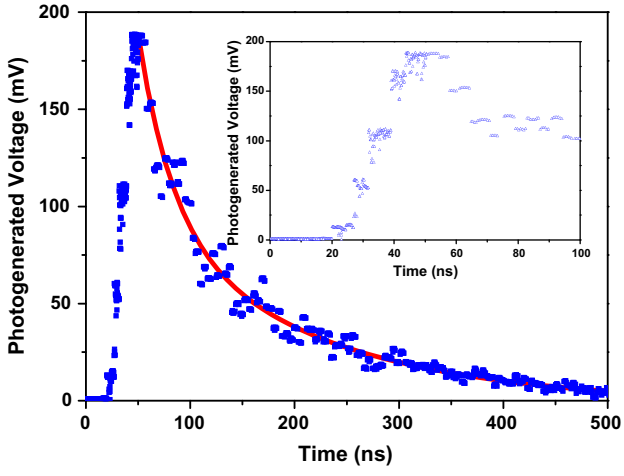

Fig. 5. Response time spectra of ZnO UV detector with the pitch of 2 μm. The inset shows the enlarged impulse response.

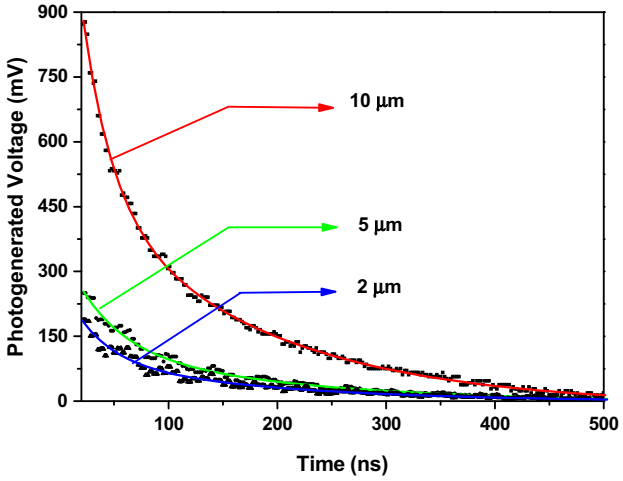

Fig. 6. The fall time with the pitches of 10 μm, 5 μm and 2 μm.

film, the time response, τ, of the MSM detector can be limited by the carrier transit time, t_{tr}, or by the RC time constant [20]

$$\tau = \sqrt{t_{tr} + (RC)^2} \tag{5}$$

where C is the sum of the detector internal capacitance and the load capacitance, R is the load resistance and the series resistance of the device. Time response was limited by RC time constant when the pitch was narrow. On the contrary, it was limited by transit time. But the surface of ZnO thin film was damaged during the device processing, and there were many trap states at the interface. So it was necessary to analyze the cause of the fall time again. The detector capacitance was estimated to be 1 pF and was confirmed by the actual capacitance–voltage measurement. Thus the RC limit was ruled out. The transit time can be estimated by [20]

$$t_{tr} = \frac{S}{V_{sat}} \tag{6}$$

where S is the pitch and V_{sat} is the hole saturation velocity. Unfortunately, to our knowledge, there are no published experimental data for carrier drift velocities in ZnO. The parameters may vary drastically due to differences in crystal growth technique. So we are unable to calculate the transit time exactly. We changed different pitches order to consider the effect of the transit time on the fall time. As shown in Fig. 6, the fall time was pretty much similar to the pitches of 10 μm, 5 μm and 2 μm. So the transit time was not the main factor of the fall time. Therefore, we attribute the fall time to the trapping of hole carriers which caused the big gain.

4. Conclusions

In summary, we have demonstrated that the Schottky type ZnO UV detector was fabricated on SiO_2 substrate by rf magnetron sputtering method. The Au-electrodes of MSM structure with interdigitated configuration were prepared by lithography and wet etching. The present results show that the big gain is due to the hole traps and it is the main factor of the fall time while the interface of ZnO thin film is not very good. With the incident wavelength of 360 nm at 3 V operating bias, the responsivity is 0.337 A/W, low dark current is 1 nA, the fast rise time and fall time are 20 ns and 250 ns, respectively.

Acknowledgements

This work is supported by the Key Project of National Natural Science Foundation of China under Grant Nos. 60336020 and 50532050, and the Innovation Project of Chinese Academy of Sciences. The National Natural Science Foundation of China under Grant Nos. 60429403, 60376009 and 60506014.

References

[1] Barnes TM, Lesf J, Hand S, Fry C, Wolden CA. J Appl Phys 2004;96:7036.
[2] Kato H, Sano M, Miyanoto K, Yao T. Jpn J Appl Phys 2003;42:L1002.
[3] Mang A, Reimann K, Rübenacke St. Solid State Commun 1995;94:251.
[4] Alivov YI, Kalinina EV, Cherenkov AE, Look DC, Ataev BM, Omaev AK, et al. Appl Phys Lett 2003;83:4719.
[5] Choopun S, Vispute RD, Yang W, Sharma RP, Venkatesan T, Shen H. Appl Phys Lett 2002;80:1529.
[6] Auret FD, Goofman SA, Hayes M, Legodi MJ, van Laarhoven HA, Look DC. Appl Phys Lett 2001;79:3074.
[7] Basak D, Amin G, Mallik B, Paul GK, Sen SK. J Cryst Growth 2003;256:73.
[8] Xu QA, Zhang JW, Ju KR, Yang XD, Hou X. J Cryst Growth 2006;289:44.
[9] Liu Y, Gorla CR, Choopun S, Sharma RP, Venkatesan T, Shen H. Appl Phys Lett 2001;78:2787.
[10] Liu Y, Gorla CR, Liang S, Emanetoglu N, Lu Y. J Electron Mater 2000;29:69.
[11] Young SJ, Ji LW, Chang SJ, Su YK. J Cryst Growth 2006;293:43.
[12] Liang S, Sheng H, Liu Y, Huo Z, Lu Y, Shen H. J Cryst Growth 2001;225:110.
[13] Angadi B, Park HC, Choi HW, Choi JW, Choi KW. J Phys D: Appl Phys 2007;40:1422.
[14] Mosbacker HL, Strzhemechny YM, White BD, Smith PE, Look DC, Reynolds DC, et al. Appl Phys Lett 2005;87:012102.
[15] Hagfeldt A, Gratzel M. Chem Rev 1995;95:49.
[16] Yang W, Vispute RD, Choopun S, Sharma RP, Venkatesan T, Shen H. Appl Phys Lett 2001;78:2787.
[17] Shur M. Physics of semiconductor devices. Englewood Cliffs, NJ: Prentice Hall; 1990.
[18] Duboz JY, Reverchon JL, Adam D. J Appl Phys 2002;92:5602.
[19] Sze SM. Physics of semiconductor devices. 2nd ed. New York: Wiley; 1981.
[20] Monroy E, Palacios T, Hainaut O, Omnes F, Calle F. Appl Phys Lett 2002;80:3198.